MONTHLY WEATHER REVIEW
VOLUME 97, NUMBER 7
JULY 1969

UDC 551.576.11:551.577.11:551.574.1:551.509.617

MODELS OF PRECIPITATING CUMULUS TOWERS

JOANNE SIMPSON and VICTOR WIGGERT
Atmospheric Physics and Chemistry Laboratory, ESSA, Miami, Fla.

ABSTRACT

This paper presents a model of the growth of cumulus clouds. The water content and maximum height of rising towers are calculated using a buoyancy equation with consideration of effects of entrainment and water load. The latter is subject to effects of modeled microphysical effects. Precipitation growth is parameterized in terms of an autoconversion equation and a collection equation. A precipitation fallout scheme is devised that depends on water content, drop spectrum, and the vertical rise rate of the tower.

Then "freezing subroutines" are devised to model the effects of silver-iodide seeding. A hierarchy of seeding routines, using different ice collection efficiencies and terminal velocities, is partially tested against the data of the Stormfury 1965 tropical cumulus-seeding experiment.

Some preliminary numerical experiments on warm clouds are performed, assuming changes in drop spectra from hygroscopic seeding.

1. INTRODUCTION

This paper reports a first step toward a long-standing goal, namely the joint dynamical-physical modeling of a cumulus cloud. The growth and fallout of precipitation interacts with the updraft, which in turn controls the amount and development of hydrometeors. The most sophisticated models of precipitation growth (e.g., Telford, 1955; Twomey, 1964; Berry, 1967) have assumed a fixed water content and invariant or zero motion field. Few dynamical models have yet considered the effects of variable fallout upon either the ascent rates or subsequent particle growth.

Kessler (1959, 1961, 1963) pioneered in introducing the effect of varying updraft into cloud physics. He evolved parameterized equations for precipitation growth. He used these equations in combination with assumed vertical motion profiles and an assumed water generation function, set to approximate adiabatic condensation. We adopt his physical approach, introduced into a simplified model predicting dynamical variables as a function of environment and cloud-base conditions.

This model is a direct outgrowth of model EMB 65 (Experimental Meteorology Branch, 1965) of an entraining cumulus tower, discussed by Simpson et al. (1965). That treatment bypassed the cloud physics by arbitrarily dropping out one-half of the liquid water condensed, regardless of updraft speed or particle spectrum. Here, we introduce the basic concepts of Kessler regarding precipitation growth, summarized by him in a recent memorandum (1967). All water is initially condensed in small cloud particles which rise with the ascending air. A process called autoconversion creates some precipitation-sized particles, which then continue to grow by collecting small cloud particles. Precipitation-sized particles have a specified terminal velocity and continually fall out of the cloud tower. The fallout relieves some of the liquid water reduction of buoyancy and acts to slow down subsequent coalescence. Our cloud physics thus consists of an autoconversion equation, a collection or coalescence equation, a terminal velocity law, and a fallout scheme.

At all stages, the model development has been tested against field measurements on both natural and artificially modified clouds. Silver-iodide seeding experiments have been particularly useful tests of cumulus models; the 1965 Stormfury series is particularly emphasized here (Simpson, Simpson, Stinson, and Kidd, 1966; Simpson, Brier, and Simpson, 1967). This modeling effort is designed to parameterize complex processes in such a way as to give realistic predictions of measurables, such as vertical tower growth, buoyancy, hydrometeor distribution, radar reflectivity, etc., in both seeded and unseeded cumulus towers.

A contrasting approach is exemplified by the brave attempts at much more sophisticated models (e.g., Ogura, 1963; Murray and Hollinden, 1966; Arnason, Greenfield, and Newburg, 1968) which integrate the full hydrodynamic equations of motion on a space grid in a series of time steps. So far, none of these have achieved sufficiently realistic relationships between vertical growth, buoyancy, size, velocity, and temperature for useful prediction in modification experiments. Among the major problems are the intractability of formulating turbulent entrainment, the limitations imposed by working within confined boundaries, errors and fictitious results introduced by finite-differencing schemes, and the restriction to two-

dimensional or axisymmetric coordinates. All these difficulties have been bypassed in the EMB series by observationally guided parameterizations so that the models give realistic and useful results despite their obvious crudities. We hope that the full hydrodynamic models can build upon the more successful of our parameterizations as the recent work by Arnason et al. (1968) has built upon those of Kessler.

2. DYNAMIC ASPECTS OF THE MODEL

The development of the numerical model, up to the EMB–65 version, is described in detail by Simpson et al. (1965). It involves integrating a differential equation for the vertical acceleration of a cumulus tower, where the acceleration is formulated as the difference between a buoyancy term and a drag term. Turner (1962) showed that the same form of the equation is applicable whether a cloud tower is idealized as a jet, a buoyant rising plume, or a "thermal" with vortical internal circulation. With the basic postulate that the internal circulation takes one, or a hybrid, of these forms, the differential equation for the rate of rise w is as follows:

$$\frac{dw}{dt}=w\frac{dw}{dz}=\frac{d}{dz}\left(\frac{w^2}{2}\right)=\frac{gB}{1+\gamma}-\frac{3}{8}\left(\frac{3}{4}K_2+C_D\right)\frac{w^2}{R} \quad (1)$$

where z is height and t is time; gB is the buoyancy force per unit mass; γ is the virtual mass coefficient; K_2 is the entrainment coefficient; C_D is an aerodynamic drag coefficient; and R is the radius or horizontal half-width of the cumulus tower.

The derivation of this equation is discussed by Simpson et al. (1965), and in more detail in a thesis by Levine (1965). Here, we will emphasize the physical foundations. It is important to keep in mind that we are using a quasi-Lagrangian framework in tracing the rise of a single cloud tower and that the coordinate system follows the circulation center of the tower. Thus, the plots of w and other variables versus z represent properties of the tower as it rises through that level. The results can only be considered cloud "profiles" in the roughest sense, during the interval that a steady-state condition might be expected to prevail. This interval may be different for the thermaldynamic properties in comparison with the hydrometeors. In the cloud physics discussion to follow, we are treating the precipitation growth and fallout within and from a single vortically circulating tower, with a roughly spherical shape and radius R. We are not able to treat precipitation growth within the whole body of the cloud, nor the ultimate rainout from its base.

The cornerstone of the dynamic modeling lies in the entrainment relation hypothesized, namely:

$$\frac{1}{M}\frac{dM}{dz}\simeq\frac{0.2}{R} \text{ (laboratory result)} \quad (2a)$$

and

$$\frac{1}{M}\frac{dM}{dz}=\frac{9}{32}\frac{K_2}{R} \text{ (theoretical result).} \quad (2b)$$

The fractional entrainment rate per unit height is $(1/M)dM/dz$ where M is the mass in the rising tower. The important point is that the entrainment or dilution is inversely related to dimension, a relationship derived in laboratory experiments on convection. Although airborne measurements are still too crude to test this relationship definitively, it was supported by a series of unpublished temperature and liquid water records made by aircraft measurements of the Woods Hole Oceanographic Institution. Deductions from other aircraft measurements are apparently in conflict (Sloss, 1967).

The proportionality constant in (2a) was found by Turner (1962) for laboratory plumes while (2b) was derived by Levine (1959) for a buoyant spherical vortex. The quantity K_2 is evaluated from equation (2b) as 0.71; if necessary, this value can be adjusted from observational tests. The radius R of the cloud tower is determined empirically, from photogrammetry or aircraft penetrations. Together with an environment sounding and conditions at cloud base, this completes the input to the numerical calculation. Over the oceans, cloud-base conditions are assumed to be saturation at environment temperature at the observed cloud base when available, or otherwise at the lifting condensation level. Over land, cloud-base temperature excesses must be known, since results are sensitive to as little as 0.5°C variation. On the other hand, the predictions are highly insensitive to the input ascent rate w at cloud base (Andrews, 1964), which is taken as 1 m sec^{-1} throughout this work.

Thus for the oceanic cases considered here, the entire calculation could be made when the sounding becomes available, without reference to the actual clouds, with the exception of the tower radius R. The necessity for measuring R on the experimental clouds is a major shortcoming of this approach, since, so far, meteorologists have no way of predicting the cloud dimensions that a given situation will produce. Nor have the more sophisticated hydrodynamic models successfully faced this problem; an input initial dimension is still required. Here, we try to pick a characteristic active tower size for each cloud. As seen in equation (2), this size selection is merely a device to determine the entrainment rate.

To date, a constant R with elevation has proved adequate. Above about 400 mb in the Tropics, entrainment becomes a less important brake on cumuli, due to lower saturation compared to actual mixing ratios. Hence, changes in R become decreasingly important with height.

The buoyancy term is evaluated as follows:

$$\text{buoyancy}=gB=\frac{g[\Delta T_v-\Delta T_v\,(\text{LWC})]}{T_v\,(\text{env})} \quad (3)$$

where ΔT_v is the virtual temperature difference between tower and surroundings and ΔT_v(LWC) is the reduction due to the weight of suspended liquid water, as formulated by Saunders (1957), namely,

$$\Delta T_v\,(\text{LWC})=T_v\cdot\text{LWC} \quad (4)$$

TABLE 1.—*Parameters of the EMB cumulus models*

Parameter	Meaning	EMB 65	EMB 68	Remarks
K_2	Entrainment	0.55	0.65	Lab. value 0.71
C_D	Aerodynamic drag coefficient	0.506	0	Solid-sphere value=1.125
γ	Virtual mass coefficient	0	0.5	Lab. value 0.5
LWC	Liquid water retained	½ condensate	Falloutscheme	Much improved in EMB 68

where T_v is the cloud virtual temperature and LWC is its liquid or solid water content in grams per gram.

Ideally, mixing and condensation should be calculated at each height step, followed directly by the buoyancy determination and integration of equation (1). The cost and complexity of this procedure has led us, however, to the simpler method involving an entrainment calculation following the method of Stommel (1947) which is independent of (1). First, the entrainment calculation is performed on the computer, proceeding from cloud base upward between sounding points and assuming in-cloud saturation with respect to either water or ice. Output variables are cloud temperature, specific humidity, and liquid water condensed. These cloud properties are then available to calculate buoyancies at any interpolated vertical intervals in order to integrate equation (1) in ascending steps. To complete gB and undertake the integration, it remains only to specify γ, C_D and a fallout scheme for the condensation products. The maximum top height achieved by the cloud is defined to be that level where w goes to zero.

Table 1 shows the specification of dynamic parameters in the EMB–65 version of the model, which was prescribed in advance of the 1965 Stormfury cumulus-seeding experiments, and the modifications made in the current EMB 68.

A major weakness in EMB 65 was the arbitrary assumption that one-half the liquid water condensed in the entrainment calculation has fallen out of the tower at each level. A fixed fractional fallout precludes any feedback between the model's physical and dynamical processes and prevents the model from even a crude prediction of precipitation growth.

With this limitation, K_2 was prescribed in the range 0. 55–0. 65 by numerous in-cloud temperature measurements, up to and including those from the Stormfury 1963 seeding experiments. A small value of C_D was introduced to allow for the apparently greater vertical-momentum reduction than that due to entrainment. Turner (1964) suggested that a virtual mass coefficient would have achieved this end more realistically. However, since EMB 65 so mishandled the water retention, it did not appear worthwhile to refine the momentum relationships further until this weakness was ameliorated. It is clear that a smaller entrainment rate and a larger fractional retention of liquid water would have equally satisfied the momentum relations, but reducing the entrainment would have given in-cloud temperature excesses higher than those observed, and so was precluded.

Despite its oversimplifications, EMB 65 gave an excellent prediction of the maximum cloud-top heights of the Stormfury 1965 seeding experiment and the growth or nongrowth of the seeded clouds (Simpson et al., 1967). The average absolute error in height prediction was only 166 m for unseeded clouds and 336 m for seeded coluds. These "errors" are within the accuracy to which top heights could be measured. Since cloud-top heights varied widely, often on the same day, this result supports the $1/R$ entrainment relation as a useful first approximation. The model was also used by McCarthy (1968) to predict seedability distributions for Project Whitetop clouds in Missouri.

3. CLOUD PHYSICS ASPECTS OF THE MODEL

Since the 1965 experiments, an improved version of the model has been developed, using parameterized equations for the growth and fallout of precipitation. This model series is called EMB 68. An intermediate model called EMB 67 was discussed by Simpson et al. (1968). It contained an error in logic in water budgeting, leading to the exhaustion of cloud water in some seeded clouds and hence will not be included here. The only important change in the dynamics from EMB 65 just described lies in the introduction of a virtual mass coefficient of $\gamma = 0.5$ and the dropping of the aerodynamic drag C_D (table 1). This change was made for two reasons. First, Turner's (1963) laboratory results suggested both that the turbulent boundary layer was continually swallowed by the rising convection element so that C_D should be zero and that a virtual mass effect arose from the pushing of outside air around the rising plume. Turner measured a laboratory value of γ of about 0. 5. Second, EMB 65 predicted too high ascent rates for the towers, at least in comparison with our somewhat fragmentary photogrammetric measurements. Use of virtual mass instead of C_D reduces rise rates while giving slightly higher cloud-top heights for the same bouyancy so that we could raise K_2 to 0.65 in the EMB–68 series. The latter figure is still consistent with the in-cloud temperature measurements and is now within 10 percent of the laboratory value of 0. 71. The figures in section 8 show that all EMB–68 cases have considerably lower and more realistic ascent rates than did the corresponding calculations in EMB 65.

The main improvement in EMB 68 is that precipitation growth is predicted, and its fallout interacts with the vertical motions. All water is first condensed as cloud water, with small drop size (roughly 5–30μ) and negligible terminal velocity. Then a process called autoconversion begins. This involves the formation of precipitation particles either by the aggregation of several cloud particles or by the action of giant salt nuclei, or similar processes. We reconsider autoconversion in relation to ice growth by vapor diffusion (Bergeron effect) later in section 6. We have used two different autoconversion equations in most

of the EMB–68 cases, namely:

$$\frac{dM}{dt}\,(\text{autoconversion}) = K_1(m-a) \qquad \begin{matrix}\text{gm m}^{-3}\text{ sec}^{-1}\\ (m>a)\end{matrix} \qquad (5)$$

or

$$\frac{dM}{dt}\,(\text{autoconversion}) = \frac{m^2}{60\left(5+\frac{.0366}{m}\frac{N_b}{D_b}\right)} \qquad \text{gm m}^{-3}\text{ sec}^{-1} \qquad (6)$$

where equation (5) is due to Kessler (1965) and equation (6) is due to Berry (1968*a*). In both equations dM/dt is the rate of growth of the precipitation water content M in gm m^{-3} and m is the cloud water content in gm m^{-3}. Kessler's linear equation was obtained intuitively. The parameter K_1 is the reciprocal of the $1/e$ "conversion time" of the cloud water. Kessler chose K_1 as 10^{-3} sec^{-1} to be consistent with a cloud lifetime of about 1000 sec. Existing cloud data probably preclude values one order of magnitude higher or lower. The "a" is a threshold cloud water content at which conversion is hypothesized to begin; we have followed Kessler in taking $a=0.5$ gm m^{-3}.

Berry's equation (6) is developed theoretically from a model of initial cloud growth by condensation and coalescence of cloud-sized particles with each other. The early droplet spectrum near cloud base has a number concentration of N_b drops per cm^3 and a relative dispersion D_b due to the condensation spectrum. The relative dispersion D_b is defined as:

$$D_b = \frac{\text{standard deviation of droplet radii}}{\text{mean droplet radius}}. \qquad (7)$$

The derivation of Berry (1968*a*) used the collection efficiencies of Shafrir and Neiburger (1963). Subsequently, Berry (1968*b*) has redone the calculation for the Davis and Sartor (1967) collection efficiencies and, at our request, has modified his parameterization formula to suit a boundary of 200-μ diameter between cloud and precipitation particles. His thus modified values are given in equation (6). The choice of the 200-μ boundary between cloud and precipitation was made for three reasons: 1) a drop with 200-μ diameter has a terminal velocity of 1–2 m sec^{-1} and is thus beginning to fall at a speed comparable to cumulus updrafts, 2) our aircraft foil precipitation sampler fails to size reliably drops much smaller than this, and 3) most 10-cm radars begin to show an echo of a cloud when numerous drops of about this size are present.

An important feature of Berry's equation is that a different autoconversion rate is predicted for maritime and for continental clouds. For maritime clouds we have chosen a drop concentration of 50 cm^{-3} at cloud base and a relative dispersion of 0.366. For extreme continental clouds we later use a drop concentration of-2000 cm^{-3} and the smaller spectral dispersion of $D_b=0.146$. These numbers are consistent with measurements by Squires (1958), Battan and Reitan (1957), and MacCready and Takeuchi (1965, 1968).

For the main comparison with the 1965 seeding data, only the maritime formulation is used. Although Kessler's equation is linear and Berry's approximately cubic, the predicted physics and dynamics of the clouds differ little enough that observational selection between them is difficult with existing data. By and large, it appears that the models using Berry's autoconversion formula give somewhat better height predictions and more reasonable liquid water distributions, although observational tests of the latter are inadequate to date.

Twomey (1959), Braham (1968*a*), and others have postulated that the entire history of coalescence precipitation growth in a cumulus is largely controlled by the initial droplet spectrum at cloud base. Use of equation (6) in our physical-dynamical model permits a fascinating test of this hypothesis in section 10.

The coalescence or collection rate is that derived by Kessler (1965, 1967) with the assumption that the precipitation spectrum follows that of Marshall and Palmer (1948). The Marshall-Palmer spectrum is defined by a single parameter n_0, namely:

$$n_D = n_0 e^{-\lambda D} \qquad (8)$$

where D is the diameter, $n_D\delta D$ is the number of drops with diameter in the range between D and $D+\delta D$ in unit volume of space, and n_0 is the value of n_D for $D=0$. The exponent λ is related to the precipitation water content by integrating over all diameters to obtain

$$\lambda = 42.1 n_0^{0.25} M^{-0.25} \qquad (9)$$

or

$$\lambda = \frac{3.67}{D_0}$$

in the gram-meter-second system of units. D_0 is the median volume drop diameter or the diameter which divides the distribution into parts of equal water content.

We use the following equation for terminal velocity of raindrops, namely:

$$V = -130 D^{1/2} \text{ m sec}^{-1} \quad (D \text{ in meters}). \qquad (10)$$

This equation was developed by Kessler (1965) from Gunn and Kinzer's (1949) data in the "Smithsonian Meteorological Tables" by List (1951). It gives slightly different values from those in the empirical table by Mason (1957). Both were used alternatively in the trial stages of our model with undetectably different results.

Using equations (8) through (10) and physical reasoning, Kessler obtains a collection equation, namely:

$$\frac{dM}{dt}\,(\text{collection}) = 6.96\times 10^{-4} E n_0^{0.125} m M^{0.875} \quad \text{gm m}^{-3}\text{ sec}^{-1} \qquad (11)$$

where E is the collection efficiency of precipitation particles for cloud particles, with a value near unity for liquid clouds. Thus the collection rate depends on the

cloud water content m, precipitation water content M, and two parameters n_0 and E.

From the Marshall-Palmer spectrum, a terminal velocity V_0 as a function of M is derivable as follows:

$$V_0 = -38.3 n_0^{-0.125} M^{0.125} \text{ m sec}^{-1}. \quad (12)$$

Physically, V_0 is the terminal velocity of the median volume drop size D_0. We also compute and print out the median volume diameter of the precipitation particles from

$$D_0 = \frac{V_0^2}{130^2} \text{ meters} \quad (13)$$

or

$$D_0 = .087\ n_0^{0.25} M^{0.25} \text{ meters}$$

for comparison with aircraft measurements.

The fallout scheme is now simple to design. We consider the average precipitation particle to be located at the tower center and to fall with terminal velocity V_0. It leaves the vortically circulating portion of the tower after falling through a height interval R. The fractional fallout of precipitation M in each height interval is therefore the ratio of the time for the tower to rise through the vertical height step over which the integration is being made (50 m) to the time for the volume median diameter drop to fall through one radius. Clearly, the larger the drops and the weaker the rise rate, the greater the fallout per unit height. Several other fallout schemes were attempted; but so far, only this one has given both consistent and realistic results.

From this point, the water-budgeting is straight forward. All water condensed in the Stommel entrainment calculation in each vertical interval $(z_2 - z_1) = dz$ is first put into cloud water m. Then autoconversion and collection calculations are applied to obtain ΔM in the interval where $dt = dz/w_1$. Then ΔM is added to M and subtracted from m. Finally, a fallout calculation is applied to obtain ΔM fallout, which is subtracted from M. The fallout is summed with height in a separate column to give later the total rainout from the tower. The final sum of $m + M$ after conversion, collection, and fallout is used in the buoyancy correction to calculate w_2, and this same sum is then exported upward to repeat the water budget in the next height interval.

The basic assumption in the cloud physics modeling is that the Marshall-Palmer (1948) spectrum, or some similarly tractable distribution, prevails for precipitation continuously during the active life of the tower. If true, this implies that the cloud processes are always restoring this spectrum in the face of the continuous fallout of the larger drops.

4. AIRCRAFT DETERMINATION OF MODELING PARAMETERS

A cooperative five-aircraft cumulus program was carried out in the vicinity of Puerto Rico in July 1967. Participants were from ESSA, the Naval Research Laboratory, and Meteorology Research, Incorporated, with dropsonde support provided by the U.S. Air Force.

The main purposes of the program were investigation of natural glaciation in tropical cumuli and measurement of the cloud-physics properties of actively rising towers. Droplet spectra were measured on the M.R.I. Piper Aztec using a foil sampler (MacCready and Takeuchi, 1967), and liquid water contents were determined by joint use of several instrument systems.

A major pertinent result was the testing of the Marshall-Palmer spectrum. Roughly, a dozen excellent penetrations through actively rising oceanic towers were obtained. The Marshall-Palmer spectrum verified to a good first-order approximation, as it also has verified in similar measurements in Project Whitetop clouds in Missouri (Braham, 1968*b*). In all cases, n_0 was 10^7 m^{-4} or slightly less; in no case would a larger value have been realistic.

With n_0 specified as 10^7 m^{-4}, sets of trial model runs were made on some of the July 1967 clouds and on the unseeded and preseeded clouds of the 1965 experiment and compared with all pertinent observations. A K_2 of no larger than 0.65 was confirmed; at least half the clouds would not reach observed levels with a higher value. The collection efficiency E in equation (11) is chosen as 1, following Kessler. Present modeling and observational deficiencies are such that adjusting it for unfrozen clouds would not be meaningful. The values of the cloud physics parameters used for all EMB–68 liquid clouds are shown in table 2.

TABLE 2.—*Cloud physics parameters for liquid clouds*

Parameter	Meaning	Value	Remarks
K_1	Autoconversion parameter	10^{-3} sec^{-1}	Kessler value
a	Autoconversion threshold	0.5 gm m^{-3}	Kessler value
D_δ	Spectrum dispersion	0.366 maritime, 0.146 continental	Berry values
N_b	Particle concentration at cloud base	50 cm^{-3} maritime, 2000 cm^{-3} continental	Observed (see text)
n_0	Marshall-Palmer intercept	10^7 m^{-4}	Observed
E	Collection efficiency precipitation for cloud	1	Kessler value

5. RADAR ECHO PREDICTION AND PRELIMINARY TEST OF MODEL

Once the precipitation water content and spectrum are defined, the radar reflectivity

$$Z = \Sigma n_D D^6 \delta D \quad (14)$$

is readily predicted, namely:

$$Z = 3.2 \times 10^{-9} n_0^{-0.75} M^{1.75} \quad (\text{meters}^3) \quad (15)$$

or

$$Z = 3.2 \times 10^{9} n_0^{-0.75} M^{1.75} \quad (\text{mm}^6 \text{ m}^{-3})$$

and when $n_0 = 10^7$ m^{-4}

$$\boxed{Z = 1.8 \times 10^4 M^{1.75} \quad \text{mm}^6 \text{ m}^{-3}.} \quad (16)$$

In EMB 68, we have also used the empirical relations between the rainfall rate R (mm hr^{-1}) and radar reflectivity Z that have been found useful in tropical areas (Gerrish and Hiser, 1964), namely:

$$R=\left(\frac{1}{68}M\right)^{1.136} \qquad (M \text{ in mg m}^{-3}) \tag{17}$$

and with

$$Z=320\,R^{1.44} \qquad (Z \text{ in mm}^6 \text{ m}^{-3}) \tag{18}$$

as found by Wexler (1947), we get

$$Z=0.322\,M^{1.6358} \qquad (M \text{ in mg m}^{-3})$$

or

$$\boxed{Z=2.6\times10^{4}\,M^{1.6358} \qquad (M \text{ in gm m}^{-3}).} \tag{19}$$

The first test of EMB 68 was made using data from a fine radar study of tropical clouds by Saunders (1965). Saunders measured radar echo intensities with a calibrated M–33 ground radar on more than a dozen warm clouds topping between 10,000–15,000 ft over the ocean near Barbados, West Indies. He also measured photographically the base and top heights of the clouds and their tower dimensions, using the radar range to establish his distance scale.

With the values in tables 1 and 2, our cloud height predictions agreed within the margin-of-measurement errors with Saunders' values, although there was a systematic overprediction averaging about 600 m or roughly 17 percent. Calculated radar echoes with equation (16) agreed very closely with Saunders' values, their average departing from his by less than 1 db. Calculated radar echoes with equation (19) averaged about 1 db higher, or not differing from the theoretical result enough to be differentiated by the average calibrated radar. Hence, we have used equation (16) throughout this paper.

6. PROBLEMS IN DESIGN OF SUPERCOOLED SEEDING ROUTINES

Design of the supercooled seeding subroutine for use with model EMB 65 was relatively simple and successful from the outset. The latent heat from one-half the condensed water was released linearly between the levels of −4°C and −8°C in the seeded cloud. The seeded cloud also proceeded from water to ice saturation in this interval.

With the physical processes introduced as in EMB 68, the design becomes more complex and difficult, with many more degrees of freedom. Furthermore, successful results are far more sensitive to the choice of parameters. The latter difficulty is more of a longrun benefit than disadvantage, since it means that seeding experiments become a sensitive tool to evaluate cloud physics processes and parameters that are very difficult to measure directly.

Conferences were held with numerous experts to consider what values should be assigned to the constants in table 2 during and after seeding. Knowledge was both scanty and conflicting; measurements at heights above the −10°C level are particularly rare, and the few sets that do exist do not include enough simultaneously measured variables to test a model. Even the forms or habits of the ice particles are not well documented. Columns and large graupellike mixtures, together with junk ice, appear to be common near −4°C (Braham, 1964; Ruskin, 1967) while columns may be replaced by some hexagonal plates between −9°C and −13°C (Todd, 1965). In tropical clouds no measurements exist to tell us whether true snow crystals appear at higher levels.

Due to the uncertainties described, we have tried a hierarchy of 24 seeded cloud models, designated as models EMB 68A through EMB 68M, with subscript K for Kessler autoconversion and B for Berry autoconversion. The models and their results are summarized in table 3, to be discussed in the following. Each combination of the physical parameters is based on a reasonable hypothesis about the structure and processes in seeded clouds. The hypotheses are tested by comparing the model results with each other and with observations.

Kessler's (1967) calculations and our own demonstrate that when collection has become active in a cloud, autoconversion may be neglected as a precipitation-forming process. Hence, in models A through K we do not modify the autoconversion equations in a glaciated cloud. In these models we do not explicitly include the Bergeron process, although this process could be physically very important in early particle growth. According to Byers (1965), diffusion growth is important only as an initiating mechanism. Once a size is attained representing an appreciable terminal velocity, coalescence becomes the predominating mechanism. Hence in models A through K, we implicitly assume that the Bergeron process could be altering our cloud spectrum m in such a way as to increase collection efficiency E in equation (11); but aside from that, we concern ourselves mainly with the input to the collection equation (11) and with the terminal velocities of ice particles.

Kessler's autoconversion equation (5), however, is suitable for modeling the faster conversion that might result from ice diffusion. Hence, in models L and M we model the Bergeron effect explicitly with a K_1 of 4×10^{-3} sec^{-1} or a $1/e$ conversion time of 250 sec or about 4 min. Observations (Bethwaite et al., 1966) indicate indirectly that this may be an extreme value, so that a higher K_1 appears implausible at present.

We retain the Marshall-Palmer spectrum for the frozen precipitation. This assumption is weaker and less justified than it is in the case of liquid clouds. Nevertheless, preliminary calculations suggest that our model results are insensitive to the exact spectrum shape provided it has the general form of a rapid decrease in number with increasing size, which surely is the case.

Conflicting evidence prevailed on collection efficiencies of ice precipitation. Laboratory results of Hosler and Hallgren (1960) suggest that it may be much less than for water precipitation, while Weickmann (1957) shows evidence that the protuberances on snow particles may enhance their collection efficiencies above that of water particles containing the same mass. Ice collection efficiency probably depends on the forms, shapes, and wetness of the ice particles, all virtually unknown. Hence, we have run a hierarchy of ice collection efficiencies ranging from 0.1–2.0 in the EMB–68 model series. Most of our dynamical and physical results are quite insensitive to this very large variation, which retrospectively justifies our rather crude parameterization of precipitation growth in an ice cloud.

The model predictions are actually much more sensitive to the ice terminal fall velocity, which exerts a stronger control on the hydrometeor retention in the cloud. We have tried terminal velocities of 20, 50, and 100 percent relative to water particles of the same mass. The 20-percent value is hypothesized roughly to represent snow crystals and flakes (Weickmann, 1957); the 100-percent value represents frozen drops, junk ice, and possibly graupel (Braham, 1964). The 50-percent cases are supposed to typify some mixture of these forms.

In our physical modeling of a frozen cloud, we use equations (10)–(12) exactly as in a liquid cloud, adjusting E and V_0, as stated above, to be characteristic of ice. In the Marshall-Palmer spectrum, D is now the "equivalent water diameter" or diameter of an equivalent mass water drop. The particle number is thus obtained, with D and D_0 merely artifacts to calculate V_0. The quantity V_0 is then reduced by any factor desired to approximate roughly the fall rate appropriate to the ice shape present.

7. THE EMB–68 SEEDING SUBROUTINES AND THEIR STATISTICAL TESTING

In all seeding subroutines, two in-cloud temperatures specify the levels flanking the tower's all-water to all-ice transformation; this "slush region" is here defined between −4°C and −8°C. Cloud water to ice changes proceed linearly with height in this interval, which is usually traversed in 3–5 min. In all seeding subroutines 60–100 percent of the total H_2O content at −4°C was eventually frozen, with the corresponding latent heat of fusion released linearly. The cloud also proceeds linearly from water to ice saturation in this region.

The reduced percentage of water frozen was considered for two reasons: 1) to allow for fallout within the slush region and 2) to allow for some natural freezing in the cloud before seeding (Ruskin, 1967; Sax, 1969). A posteriori calculations of fallout in the slush region showed that at −8°C most seeded clouds retained about 90 percent or more of their total H_2O content at −4°C.

We have made no change in equation (16) for the radar-reflectivity versus precipitation relationship for the seeded clouds. According to Austin (1963), for ice and snow we may use

$$Z\ (\text{ice}) = 1000\ R^{1.6} \qquad (R \text{ in mm hr}^{-1}), \quad (20)$$

while from Gunn and Marshall (1958) we find that in ice clouds

$$M = 250\ R^{0.90} \qquad (M \text{ in mg m}^{-3}) \quad (21)$$

has proved satisfactory. Combining (20) and (21) we get

$$Z\ (\text{ice}) = 0.0546\ M^{1.778} \qquad (M \text{ in mg m}^{-3}) \quad (22)$$

or

$$Z\ (\text{ice}) = 1.18 \times 10^4\ M^{1.778} \qquad (M \text{ in gm m}^{-3}).$$

Computations of Z were made and compared from (16) and (22) for numerous values of M in the range 0.5–3.0 gm m^{-3}, which corresponds to the range in our clouds. Equation (16) gives values less than 2 decibels (dB) higher than equation (22). We believe that the uncertainty in particle size and spectrum exceeds this margin, as do the calibration errors in most radars. Hence, we continue to use (16) for the seeded clouds, with the reservation that the predicted radar reflectivities for glaciated conditions should be regarded with skepticism until further measurements are available.

Table 3 describes the hierarchy of models and the statistical evaluation of each with the 1965 Stormfury cumulus data. It is important to note that so far the seeding model tests have been made (from necessity) almost entirely with dynamic properties of the clouds, using top heights in particular. In general, those models which failed badly to predict top heights also gave ridiculous water contents. Only one clearly unsuccessful model (E) is shown in table 3.

In table 3, column 1 gives the designation of the model; the subscript K or B denotes whether Kessler's or Berry's autoconversion was used. Column 2 gives the percent of the water content at −4°C assumed frozen by the seeding. Column 3 gives the ice collection efficiency E_I used in equation (11). Column 4 gives the terminal velocity V_{TI} in terms of the percent of the terminal velocity computed from equation (12). Column 5 gives the average absolute error in top height prediction for all seeded clouds, while column 6 gives the average algebraic error.

It is immediately clear that model E, with no precipitation fallout, gives preposterous results, which will be analyzed later. Of the remaining models, those with 20-percent V_{TI} clearly give better results than those with 50 or 100 percent. Regardless of the shortcomings of the models or of the exact particle spectra, it is clearly necessary that relatively more water be retained in the clouds after seeding than before, in order to prevent overpredicted cloud tops. This conclusion is clarified by the waning effectiveness of entrainment in reducing buoyancy and hence vertical ascent in the upper levels of the clouds.

TABLE 3.—*Hierarchy of models and statistical evaluation of each with the 1965 Stormfury data. See text for details.*

1 Model	2 TLWC (%)	3 E_I	4 V_{TI} (%)	5 $\lvert\bar{\varepsilon}\rvert$ (meters)	6 $\bar{\varepsilon}$ (meters)	7 $R_{S,EF}$	8 m	9 b (kilometers)	10 $\overline{\Delta R/R}$ (%)	11 $R_{P_s,\Delta R}$	12 $R_{EF,\Delta R}$
68 A_K	100	0.1	20	570	−50	0.93	0.78	+0.44	−7	−0.92	+0.79
68 A_B				520	+33	0.93	0.82	+0.24	−8	−0.92	+0.75
68 B_K	60	0.1	20	480	−380	0.95	0.86	+0.55	−7	−0.90	+0.83
68 B_B				450	−330	0.94	0.92	+0.38	−9	−0.90	+0.78
68 C_K	80	0.1	20	490	−230	0.94	0.82	+0.50	−7	−0.91	+0.81
68 C_B				440	−160	0.94	0.87	+0.30	−8	−0.91	+0.77
68 D_K	90	0.1	20	480	−150	0.94	0.80	+0.46	−8	−0.92	+0.80
68 D_B				460	−60	0.94	0.84	+0.28	−9	−0.91	+0.76
68 E_K	100	0.1	None	1140	−1060	0.24	0.28	+2.48	No fallout		
68 E_B				1590	−1510	0.23	0.28	+2.46			
68 F_K	100	1.0	100	980	+510	0.90	0.65	+0.35	+22	−0.57	+0.97
68 F_B				900	+750	0.94	0.72	−0.03	+22	−0.69	+0.63
68 G_K	100	0.1	100	730	+230	0.91	0.71	+0.39	+7	−0.85	+0.86
68 G_B				730	+390	0.92	0.73	+0.16	+11	−0.81	+0.83
68 H_K	80	1.0	100	810	+310	0.91	0.68	+0.39	+20	−0.49	+0.98
68 H_B				760	+375	0.92	0.72	+0.20	+17	−0.57	+0.97
68 I_K	100	2.0	50	940	+460	0.92	0.66	+0.37	+19	−0.56	+0.96
68 I_B				820	+470	0.92	0.70	+0.17	+14	−0.68	+0.92
68 J_K	80	1.0	50	680	+160	0.93	0.71	+0.43	+13	−0.57	+0.97
68 J_B				610	+210	0.93	0.76	+0.24	+9	−0.65	+0.94
68 K_K	80	1.0	20	480	−90	0.94	0.77	+0.48	+1	−0.83	+0.89
68 K_B				430	−50	0.94	0.84	+0.29	−4	−0.86	+0.82
68 L_K^*	80	0.1	20	480	−180	0.94	0.80	+0.49	−4	−0.89	+0.84
68 M_K^*	80	1.0	20	480	−90	0.94	0.77	+0.48	+1	−0.84	+0.89

*Fast autoconversion (Bergeron effect)

Aloft, increased water retention becomes the sole way to restrict the vertical momentum. Logically, more water retention means less fallout, which works against increased precipitation by seeding (discussed in section 8).

Columns 7–9 in table 3 relate to statistical evaluation of results, similar to that performed by Simpson, Brier, and Simpson (1967) with EMB 65 and the same data. Two quantities, seedability S and seeding effect EF, are defined. Seedability is the difference in predicted top heights between seeded and unseeded clouds. Seeding effect is the difference between the observed maximum top height and the predicted unseeded top height. Column 7, $R_{S,EF}$ is the correlation coefficient between seedability and seeding effect for all 1965 seeded clouds.

If our models and data were perfect, the correlation $R_{S,EF}$ would be 1.0 for seeded clouds, since their observed growth above the unseeded predicted top should equal their seedability. For unseeded clouds, the correlation $R_{S,EF}$ should be zero. Note that in all models (except E) the seeded correlation exceeds 0.90, which is significant to better than 1 percent. Figure 1 shows the EF versus S diagrams for models EMB 68, C_B and K_B. Graphs with similar appearance resulted from all other models except E. Seeded and unseeded clouds formed different populations, with different means and regressions. (Unseeded computations were identical for all EMB–68 models A–M, except E, no fallout. With the exception of E, the only difference between models lies in seeded parameters.) Essentially no correlation between S and EF resulted for the unseeded cases. The slightly better correlation found with EMB 65 is accounted for by clouds 7 and 12 which actually failed to grow after seeding. The EMB–68 model series underpredicted the unseeded tops of both these clouds but correctly predicted the seeded tops leading to a finite (incorrect) EF.

The high correlation $R_{S,EF}$ demonstrates a linear relationship between S and EF. Columns 8 and 9 in table 3 give the slope and intercept, respectively, of the best fit straight line to the circled points in the diagrams exemplified in figure 1. Again, perfect modeling and data would give $m=1.0$ and $b=0$. The degree to which m and b approach these values is a measure of the adequacy of the models.

Using all the measures in columns 5–9, models A–D and K–M give the best results. These are the models with ice terminal velocity only 20 percent that of equivalent mass

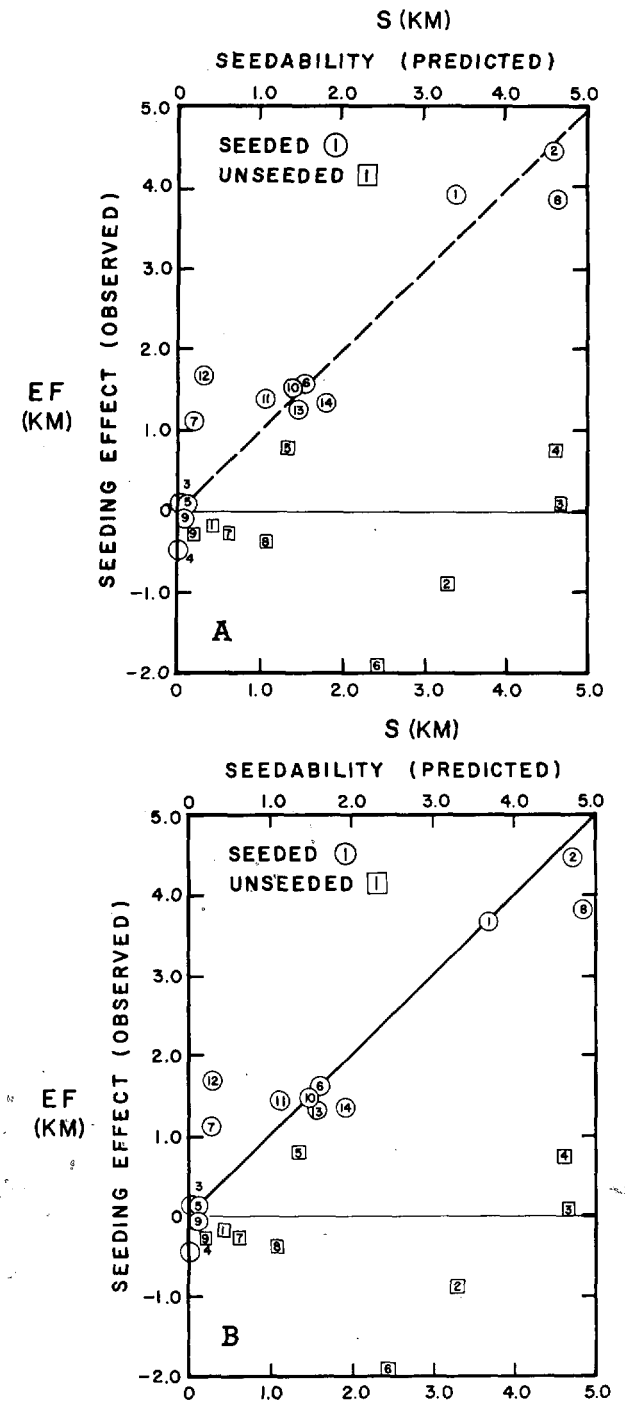

FIGURE 1.—Seeding effect *EF* versus seedability *S* (both in kilometers) for two versions of the EMB–68 model, (A) EMB 68 C_B and (B) EMB 68 K_B (see table 3 for both models). The dashed line is the theoretical curve for seeded clouds; the solid line is the theoretical curve for control clouds.

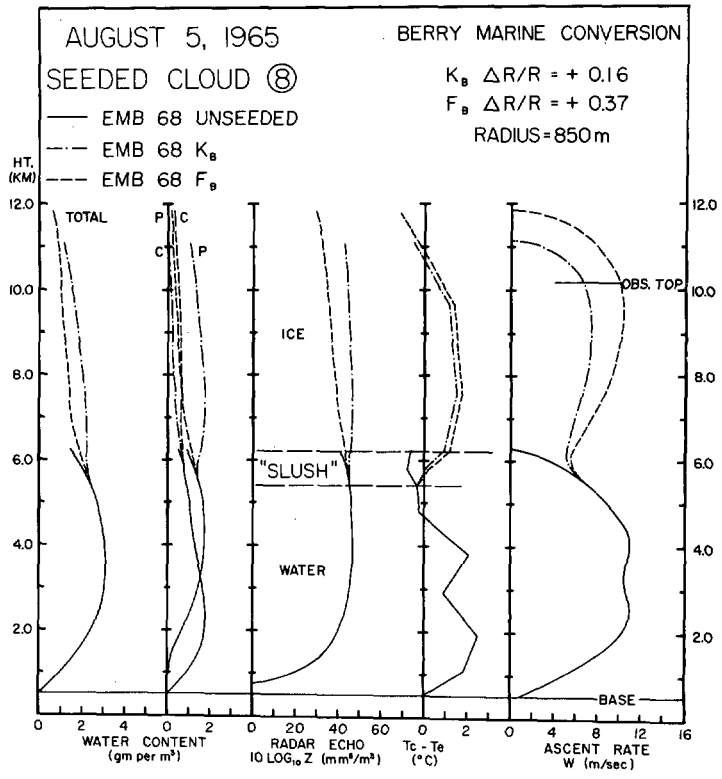

FIGURE 2.—Comparison of results for models EMB 68 K_B versus F_B for cloud of Aug. 5, 1965. The main difference between models is that F eventually freezes 100 percent of the water contained in the cloud at −4°C, while K freezes 80 percent. In F, ice particles have the same terminal velocities as water particles, while ice terminal velocity is greatly reduced in model K. The graphs give properties of the rising tower as functions of height. P stands for precipitation water content (*M* in text); C stands for cloud water content (*m* in text). ΔR is the seeded minus the unseeded fallout; *R* is the unseeded fallout. The heights are for the center of the cloud tower. Hence, the observed tops have been corrected by subtracting the tower radius.

liquid drops. Figure 2 compares, for a typical seeded cloud, results using models 68K and F. The much higher sustained water content in the more successful seeded models is evident. The difference in total H_2O content is of the order of 1 gm m^{-3}. This difference would be detectable with present instrumentation, such as the Lyman-α system with evaporator, if it could be flown into seeded cumuli at levels of 7–9 km.

In the two fast autoconversion (strong Bergeron effect) models, L_K is the same as C_K except for fourfold more rapid conversion, while M_K is the fast conversion version of K_K. The results of M_K and K_K are so nearly identical that the plotted curves and all other features are indistinguishable. The result shows that when the ice collection efficiency is 1.0 or more, even a strong Bergeron effect on conversion makes no difference and may be neglected for our present purposes. Figure 3 compares a sample case for C_K and L_K. The dynamics of the two clouds are virtually identical, hence only the physical parameters are shown. We see about 0.3 gm m^{-3} more precipitation in the L case. In large part, faster conversion compensates for reduced ice collection efficiency in seeded clouds. For this and other reasons, models A–D are probably less realistic since they reduce ice collection without allowing for the compensation by the Bergeron effect.

However, models A–D do make the important point that, within wide limits, the amount of liquid water frozen by seeding does not matter much. Model B, with 60 percent, produces as good results as model A with 100

352-162 O - 69 - 2

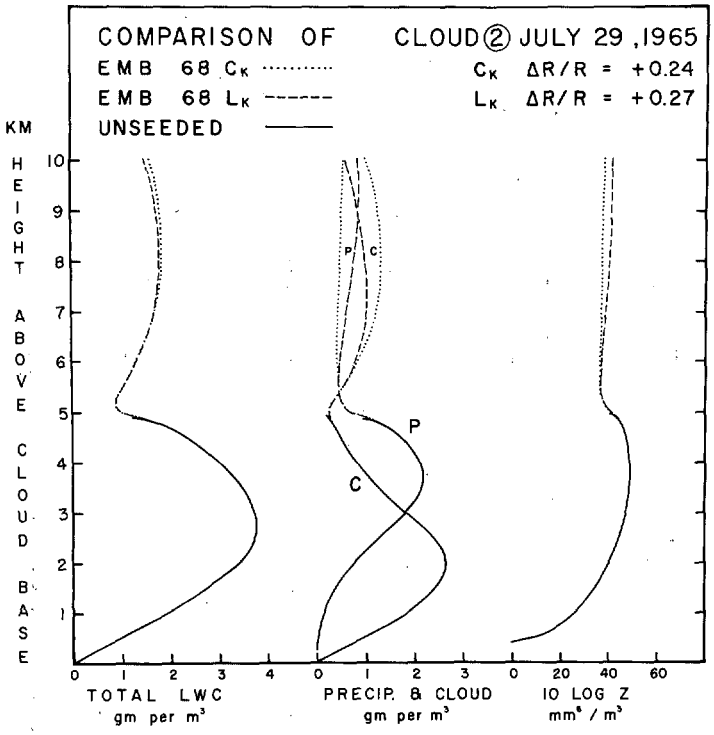

FIGURE 3.—Comparison of physical predictions by models C_K and L_K on expanded horizontal scale. Model C_K has same autoconversion rate in seeded as unseeded cloud and a 0.1 collection efficiency of ice for ice. Model L_K has the same low ice-collection efficiency but a four times faster autoconversion rate in the seeded cloud, to simulate a strong Bergeron effect. Other notation same as figure 2. Note little difference in fractional precipitation increase.

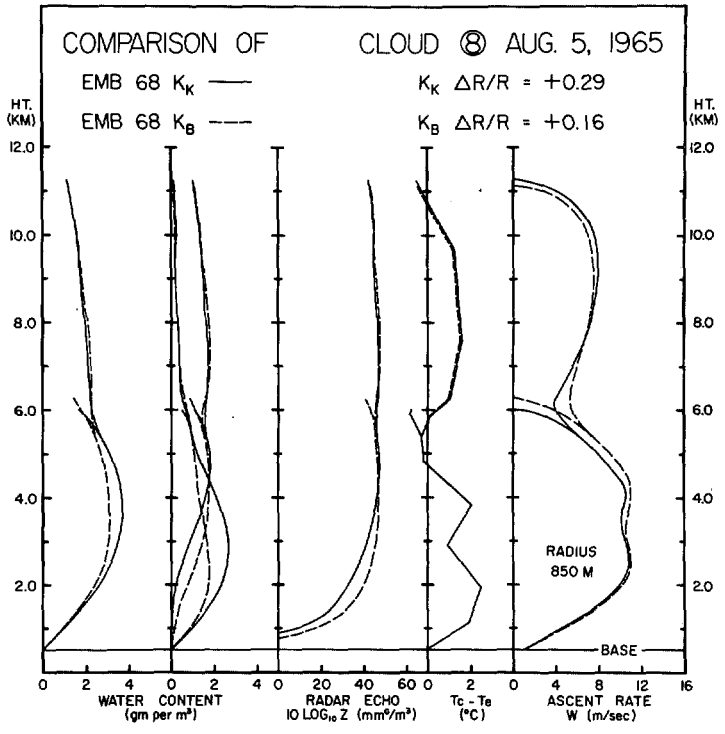

FIGURE 4.—Comparison of model results using Kessler's autoconversion (solid) versus that of Berry marine (dashed). Comparison made with model EMB 68K for the seeded cloud of Aug. 5, 1965. Note the similar end products despite faster early precipitation growth using Berry's formulation. With parameters characteristic of continental clouds (not shown), Berry's formulation leads to slower precipitation growth than Kessler's.

percent. Allowing for 10 percent fallout in the slush region, this means that as much as 30 percent of the water in the cloud updraft could be naturally frozen without much reducing the growth increases expected from seeding. Our field results (Ruskin, 1967; Mee and Takeuchi, 1968) suggest that 10–20 percent is nearer the amount of natural freezing in active updrafts between −4°C and −8°C. Hence, we choose the models eventually realizing the latent heat from 80 percent of the water contained at −4°C.

Overall, model K appears to verify best, particularly the version with Berry's autoconversion. Figure 4 shows a typical comparison of results with the two autoconversion schemes, using seeded cloud 8 on Aug. 5, 1965. While the upper portions of the tower are nearly identical in all properties, between 2–4 km the proportions of precipitation versus cloud water differ. Berry's formulation leads to earlier growth of precipitation in the rising tower than does Kessler's.

At present, we do not regard the use of an ice collection efficiency of 1.0 as implying that the ice collection process is unaltered from that of water, but rather that opposing effects possibly compensate. It is likely that reduced collection by the hardened ice surfaces is compensated both by the branches or protuberances on the ice particles and by the Bergeron effect. In any case, results are quite insensitive to reasonable variations in E_I. The greater success of the lower V_{TI} models strongly suggests the dominance of the more slowly falling crystalline forms following seeding, whether they are snowflakes, columns, or plates. Much more particle sampling needs to be undertaken in seeded clouds and at higher levels than has so far been possible.

Table 4 compares, cloud by cloud, the predicted liquid water contents at −4°C in all EMB–68 models except E (predicted unseeded water contents are identical for all models except E) with those measured by the ESSA DC–6 flying at 19,000 ft, where ambient temperatures were about −6°C to −8°C. The measuring equipment used was that described by Levine (1965).

A correlation between water content at −4°C and seeding effect was run. The correlation was −0.25, which is not statistically significant.

The complete failure of model E requires some discussion. In this model, zero fallout of precipitation was assumed from both the unseeded and the seeded towers. Cloud water was converted to precipitation using equations (5) or (6) and (11), but no water was dropped out of the tower. With this model, nearly half of the seeded clouds failed to reach the −4°C level, in contradiction to observed heights at seeding. For those that were predicted to reach the seeding level, table 3 shows that the predictions were hopelessly poor, and no significant correlation between

TABLE 4.—*Predicted and observed water contents at −4°C in 1965 seeded clouds*

Cloud	Model (gm/m³)	Obs. (gm/m³)	Remarks
① K	2.17	1.6–2.0	Several towers—average
B	1.75		
③ K	1.95	1.6–1.8	Average for seeded tower
B	2.10		
⑥ K	2.12	Missing	Aircraft passed over top.
B	2.0		
⑧ K	3.92	0.6	Aircraft missed tower. Aircraft at 10,000 ft measured 3.5 gm/m³.
B	3.30		
⑦ K	.....	Missing	Aircraft passed over top.
B	2.08		
⑧ K	2.64	1.6–2.4	See Ruskin (1967).
B	2.35		
⑨ K	2.70	Missing	Cloud did not reach aircraft level.
B	2.33		
⑩ K	2.82	Missing	No before-seeding penetration
B	2.52		
⑪ K	2.38	Missing	No before-seeding penetration
B	2.09		
⑫ K	2.46	Missing	No before-seeding penetration
B	2.39		
⑬ K	2.82	Missing	No data
B	2.61		
⑭ K	3.36	~1.8–2.1	Two towers
B	3.11		

Note: Clouds ⑤ and ④ were seeded at temperatures above 0°C and did not reach the −4°C level.

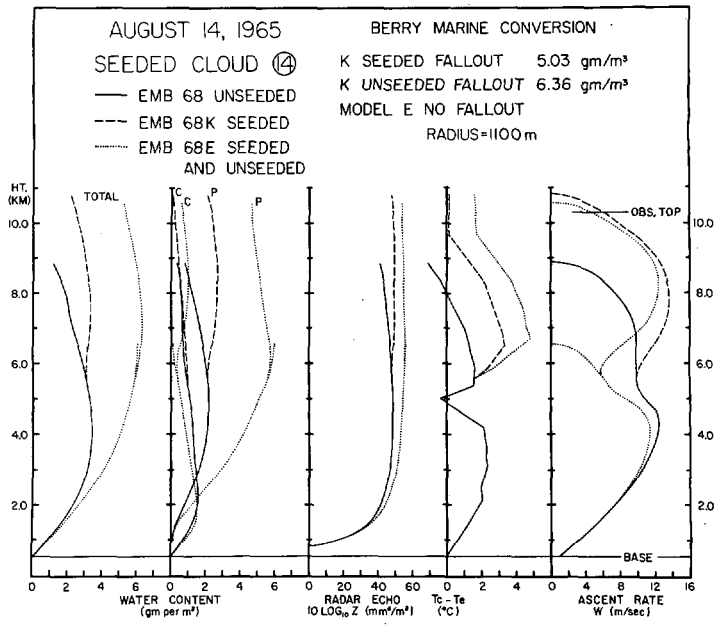

FIGURE 5.—Comparison of predictions by models EMB 68 E_B (dotted) and 68 K_B (unseeded, solid; seeded, dashed). Model E has no fallout. Note unrealistically large precipitation water and total water contents predicted by model E. The higher predicted seeded cloud temperature excess in model E is due to the higher water content and the fact that 100 percent of the water in the cloud at −4°C is eventually frozen.

seeding effect and seedability was obtained. Since no fallout of large drops occurs, the precipitation spectrum tends to larger and larger mean drop sizes and unrealistically rapid growth. From equation (11), we see that if M is too large, dM/dt will also be too large; and the error will build up with time or elevation.

Figure 5 shows a sample comparison between models E and K for the Aug. 10, 1965, case. The water content in E is nearly 6 gm m^{-3} in the slush region, compared to about 3 gm m^{-3} for model K, which was higher than the measured amount (table 4). In E, about 5 gm m^{-3} or 92 percent of the water is in precipitation. The radar echo exceeds 56 dB, and the volume median drop diameter for precipitation is 2.4 mm. In K, the corresponding values for the slush region are 3.2 gm m^{-3}, with 2.3 gm m^{-3} or 74 percent in precipitation; D_0 is 1.9 mm. The latter values are more consistent with Saunders' (1965) figures and with our own water and spectral measurements (Mee and Takeuchi, 1968).

Weinstein and Davis (1968) have used a model, in ome respects similar to E, with apparent success in predictions relating to Arizona clouds. In their model, no fallout is assumed for the cloud physics calculations of equations (10)–(16). However, for the dynamic calculation from equation (1), all water is dropped, in each height interval, that has a terminal fall speed greater than w. It is readily shown that this implies negligible fallout when w exceeds about 6 m sec^{-1}. The colder cloud base (~0°C) and continental character of Arizona clouds, however, favor smaller entrainment and higher relative water contents (Woodley, 1966). Sax (1969) has used the Weinstein-Davis model on the Stormfury 1965 cases with successful height predictions for all but cloud 1. Omitting cloud 1, the correlation $R_{S,EF}$ came out 0.92.

Closer examination, however, reveals that radii 50–400 percent larger than our values were used. For that model, R is supposed to comprise the entire cloud body. Since a comparable K_2 was used, radii this large reduce entrainment to a negligible braking effect. Thus, their height predictions are successful because of the large weights of water carried. No observational comparison of predicted in-cloud temperature excesses or water contents were made. Our earlier results (Simpson et al., 1965; Simpson, Brier, and Simpson, 1967) suggest that in-cloud temperatures would be at least 1–2°C too high if the radii are increased by 50–400 percent. Figure 5 shows that the no fallout water content is too large by a factor of about two with the correct radius; it would be still larger with a wider radius and the concomitant near-adiabatic condensation rate.

We conclude that models without fallout cannot treat precipitation growth nor cloud physical-dynamical interactions realistically enough to be useful, particularly in the case of maritime tropical clouds.

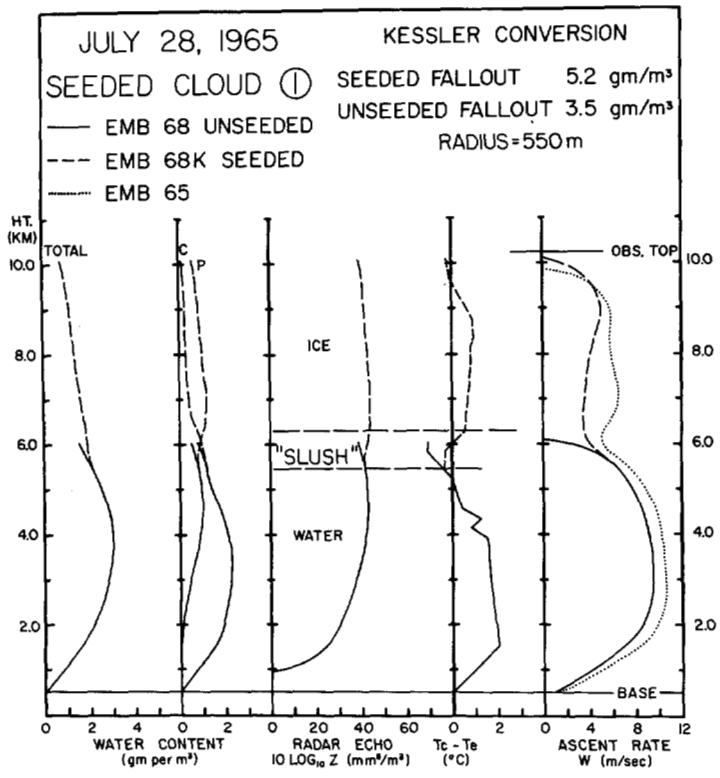

FIGURE 6.—Predicted properties of seeded cloud 1, July 28, 1965, using model EMB 68 K_K. The observed cloud (see figs. 9 and 12) grew explosively following seeding.

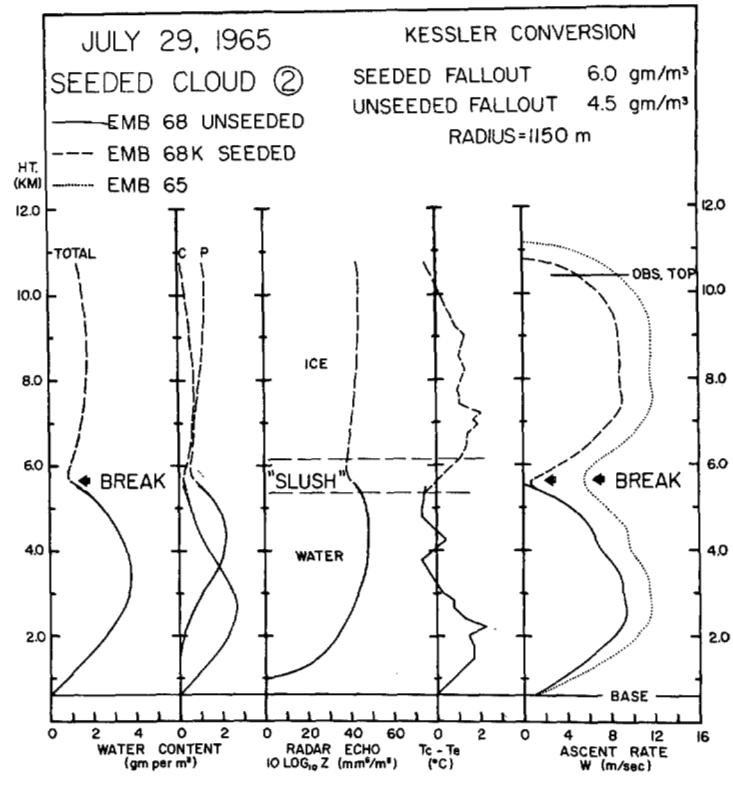

FIGURE 7.—Predicted properties of seeded cloud 2, July 29, 1965, using model EMB 68 K_K. The observed seeded cloud tower (see figs. 10 and 13) grew vertically following seeding, cutting off from the main cloud body which dissipated.

8. PRECIPITATION CHANGES FOLLOWING SEEDING AND PHYSICAL-DYNAMICAL INTERACTIONS

Columns 10–12 of table 3 deal with calculated precipitation changes between seeded and unseeded clouds. The quantity ΔR is defined as the difference in the summed fallout between the seeded and the unseeded tower, while $\Delta R/R$ is the ratio of this difference to the unseeded fallout or the fractional change in precipitation fallout due to seeding. The number appearing in column 10 is the average percentage change in fallout for all seeded clouds (except 3 and 4, which were seeded above 0° C).

The average $\overline{\Delta R/R}$ does not mean much in itself since it is composed of large increases versus large decreases, with roughly the same number of clouds showing predicted increases as decreases. Figures 6–8 illustrate this point with model K. Figures 6 and 7 show results for seeded clouds 1 and 2. In all models, these clouds showed the largest positive values of $\Delta R/R$. For example, cloud 1 (Kessler) showed a 19-percent increase in model A and a 51-percent increase in model F, the extreme cases. Figure 8 shows the results for seeded cloud 6, which showed the largest precipitation decrease. The correspond-

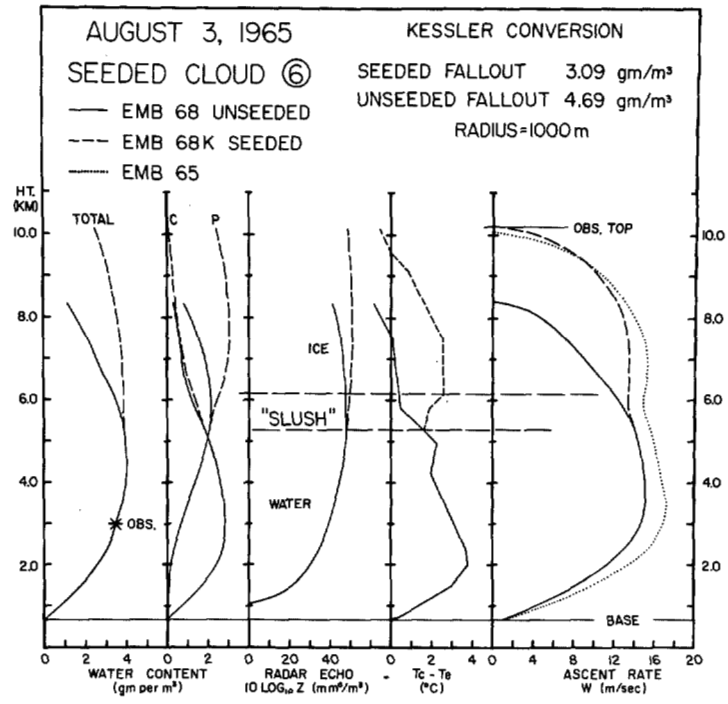

FIGURE 8.—Predicted properties of seeded cloud 6, Aug. 3, 1965, using model EMB 68 K_K. Note the relatively large top height predicted for the unseeded cloud and the smaller fallout predicted for the seeded cloud. The observed cloud (figs. 11 and 14) grew explosively following seeding.

ing range in its $\Delta R/R$ (Kessler) is from -44 percent in model A to $+12$ percent in model F. Thus, the average values should be interpreted in this light. When the average is negative for a model, it simply means smaller pluses, one or two fewer clouds with increases, and larger decreases.

Those clouds that showed large predicted precipitation increases from seeding in all models were those with low unseeded tops and large seeding effect *EF*, while those with large precipitation decreases were those with tall unseeded tops and a smaller value of *EF*. The two clouds that failed to grow (5 and 9) after seeding showed negligible precipitation change; these two are omitted from the correlations shown in columns 11 and 12. The inverse correlation between unseeded top heights and ΔR is, in nearly all models, significant at better than the 5-percent level. The positive correlation between seeding effect and ΔR is significant in all cases. Physically, this result means that if an unseeded cloud will grow naturally to heights of 8–10 km, seeding will probably decrease precipitation fallout by "hanging up" the precipitation particles in the ice phase. Little is gained by further growth above these levels since the condensation rate falls off to very small values at cold temperatures. The most promising cases for increased fallout from seeding are those clouds whose natural growth does not exceed 6–7 km and where a big seeding effect is predictable from the model.

Since ΔR denotes only the fallout difference between seeded and unseeded towers, similar calculations to those in columns 10–12 were run for total precipitation production by the towers. The results were so nearly similar to the foregoing that they are not shown.

The changes in precipitation fallout are on the order of 20–30 percent and generally in the range of about 1 gm m^{-3}. This is about half an inch over 2 sq mi, or more than 50 acre-feet. This amount is of course not much, but we are considering only the rising period of a single tower. In an explosive growth case, many towers succeed each other over a greatly prolonged lifetime, so that conceivably we could obtain the half inch over as much as three times the area, or a total of perhaps about 160 acre-feet, which is not negligible. By the same argument, of course, an explosive growth could overcome the calculated negative fallout difference computed only for the first tower in comparison with its unseeded fallout.

It should be emphasized that we are not able to compute how much of the cloud fallout reaches the ground as precipitation. This potentiality will depend upon how much of the tower fallout descends through the cloud body and how much through the drier environment, hence upon environmental circumstances such as humidity, wind shear, and cloud-base height. Nevertheless, we hypothesize a proportionality between our calculated fallouts and potential rainfall production by seeding. In other words, circumstances of explosive growths of towers which are predicted not to grow high without seeding are most favorable, while cut-off growths are less so. Clouds which are predicted to grow to the cumulonimbus or near-cumulonimbus stage, unseeded, should show the smallest gains or even rainfall losses from seeding. We plan to test this hypothesis with the results of a 1968 Florida seeding program in which the precipitation at numerous levels, from cloud base upward will be evaluated with calibrated ground radars.

Meanwhile, comparison of the clouds modeled in figures 6–8 illustrates very well the interactions between physical and dynamical features and perhaps explains some aspects of the difference between explosive growth and cut-off tower growth. Clouds 1 and 6 were observed to grow explosively following seeding, while cloud 2 exhibited the cut-off tower regime. Figures 9–11 are photographs of these clouds; figures 12–14 show their scale outlines, reconstructed photogrammetrically. Two features distinguish the cut off from the explosive cases. The first is the wider measured cloud body of clouds 1 and 6 compared to cloud 2. The second distinguishing feature lies in the calculated velocity, water, and temperature profiles. Note in figure 7 that the vertical ascent rate goes virtually to zero at 6 km, while it increases rapidly to above 8 m sec^{-1} between 7 and 8 km. The diminution of ascent rate causes a "dumping" of hydrometeors at 6 km, the level at which the break appears. The unloading of the tower permits it to accelerate rapidly, while the rather narrow cloud body below is apparently killed (fig. 10B) by the "fall-through" of the precipitation. A stable dry layer in the environment of cloud 2 gives rise to a strong negative buoyancy from just above 4 km to nearly 6 km.

9. MARITIME VERSUS CONTINENTAL CLOUDS AND WARM CLOUD EXPERIMENTS

Figure 15 shows a typical maritime tropical cumulus and its extreme continental counterpart. The same sounding and radius are used for both clouds, as is the Berry conversion equation (6). For the maritime cloud, $N_b=50$ cm^{-3} and $D_b=0.366$. For the continental cloud, $N_b=2000$ cm^{-3} and $D_b=0.146$. The dynamics of the resulting clouds are virtually identical, although the continental cloud terminates about 100 m lower due to the 1 gm m^{-3} higher water content near its top. The physical properties and radar echoes of the clouds are utterly different. The precipitation fallout is nearly eight times as much from the maritime cloud as from the continental cloud!

The vast predicted difference, particularly in precipitation, between maritime and continental clouds encourages experimentation on converting one type of cloud into the other, particularly by seeding with hygroscopic particles. Could a maritime cloud be inhibited from raining by the addition of very many small hygroscopic particles? More importantly, could a continental cloud be caused to rain more by broadening its cloud base spectrum? Figures 16 and 17 are preliminary numerical tests of these ideas.

FIGURE 9.—Photograph of seeded cloud 1, July 28, 1965, at seeding time (2217:30 GMT). Right-hand portion seeded.

In experiment 1 (fig. 16), we hypothesize adding enough small hygroscopic particles to reach the continental concentration, but since we cannot remove the giant oceanic nuclei, we leave the relative dispersion unchanged. The results are striking. We predict a large (nearly 100 percent) increase in cloud water content and a 72-percent decrease in precipitation fallout.

In experiment 2, we try to make a continental cloud more maritime and to increase precipitation by a hypothetical introduction of enough large hygroscopic particles to widen the relative dispersion to 0.488 while leaving the droplet concentration unchanged from 2000 per cm^3. The results are successful, although less so than in experiment 1. We predict an increased precipitation fallout of 150 percent per tower which, however, amounts to only 0.29 gm m^{-3} or at most about 15 acre-feet.

Thus, while hygroscopic seeding appears the most promising technique for rain increase under drought conditions, when only warm clouds are present, it is not as drastic nor as powerful a cloud modification technique as silver-iodide seeding, since it only affects the physics of the seeded tower itself, while silver-iodide seeding can affect the dynamics of the entire convective system over numerous life cycles of an individual tower.

10. CONCLUDING REMARKS

A final supercooled seeding experiment was tried numerically, designed to test the Bergeron effect alone. Dynamic effects via latent heat release were assumed to be zero, and the only seeding effect was hypothesized to be increased autoconversion beginning at −4°C in the seeded clouds. These experiments were performed with the Kessler formulation only. Values of K_1, 4 times and 10 times the value (10^{-3} sec^{-1}) used for liquid clouds, were taken. The tiny increases in precipitation and fallout were too small to affect any of the significant figures in the predictions. This result confirms an earlier

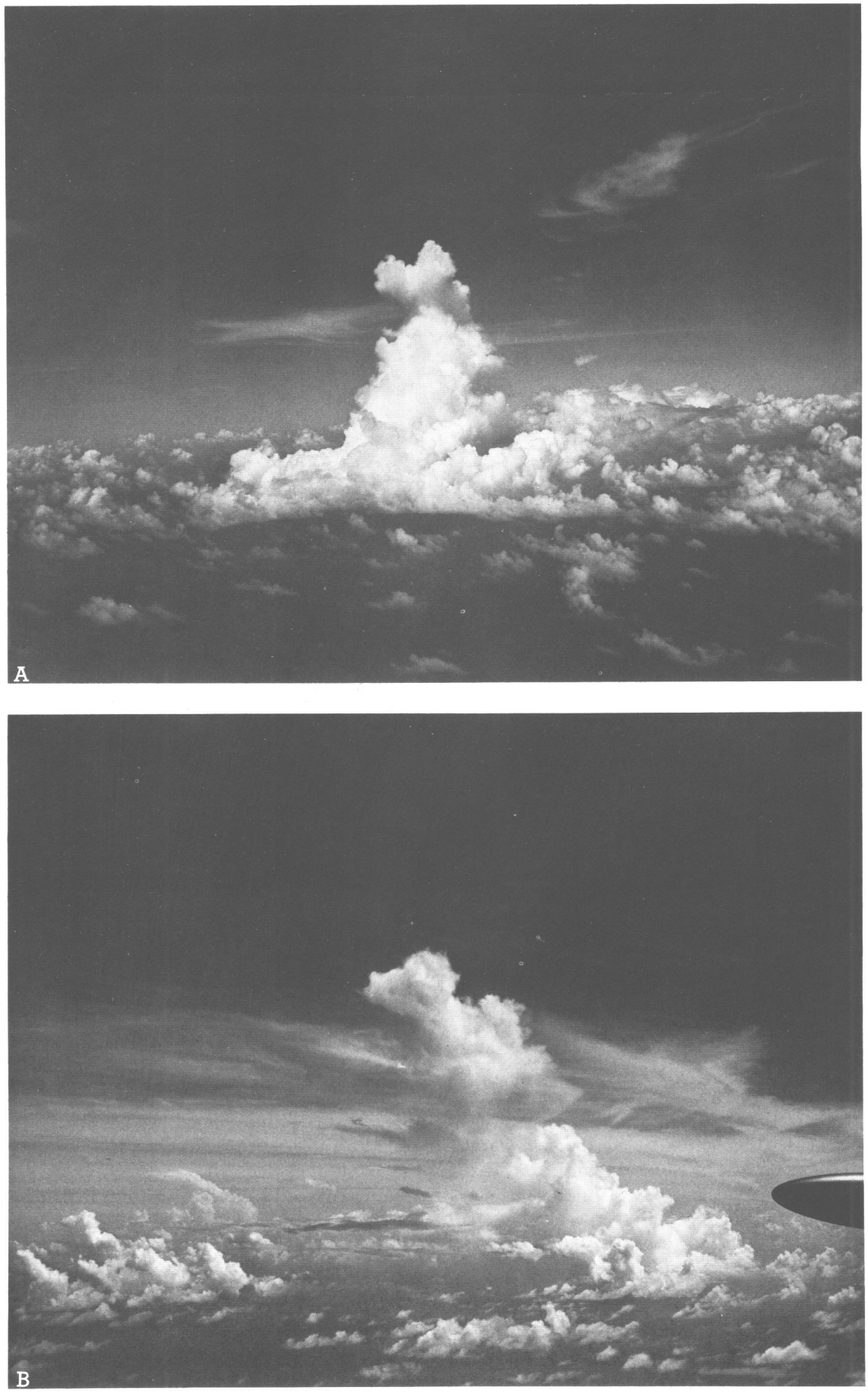

FIGURE 10.—Photographs of seeded cloud 2, July 29, 1965; (A) at 1½ min after seeding (1812 GMT); (B) at 15½ min after seeding (1826 GMT). Note that seeded tower has cut off and is showering into main cloud body below, which is dissipating.

FIGURE 11.—Photograph of seeded cloud 6, Aug. 3, 1965, at 11½ min before seeding (2147 GMT).

conclusion by Kessler (1967) that large changes in autoconversion do not affect precipitation growth after collection has become important in a cloud.

Therefore, the main conclusion of this paper is that the main effect of seeding supercooled tropical cumuli is through the alteration of the cloud dynamics, which in turn alters the water carried and precipitated. The feedback of the physics to the dynamics only changes the motion field critically in certain marginal situations, for example the cut-off case of figure 6.

A hierarchy of quite different physical models, with widely different ice collection efficiencies and ice fall speeds gives results dynamically very similar to each other. Furthermore, the results with the new EMB–68 series are qualitatively the same as with the simpler EMB–65 model—the clouds that grew significantly following seeding could not be made to fail to grow (and vice versa) with any reasonable permutations of the seeding subroutine nor of the ice regime. However, some selection among the physical models was possible with available measurements, suggesting a reduction of ice terminal velocity relative to that of water particles.

The best EMB–68 models give reasonable predictions of precipitation growth, fallout, and radar echo intensity, which stand to be tested with results of the next observational program. Both positive and negative precipitation changes of the order of 20–30 percent are predicted. These are equivalent to water amounts of 100–200 acre-feet per cloud of these dimensions, if precipitation falling from the tower reaches the ground. In any case, it

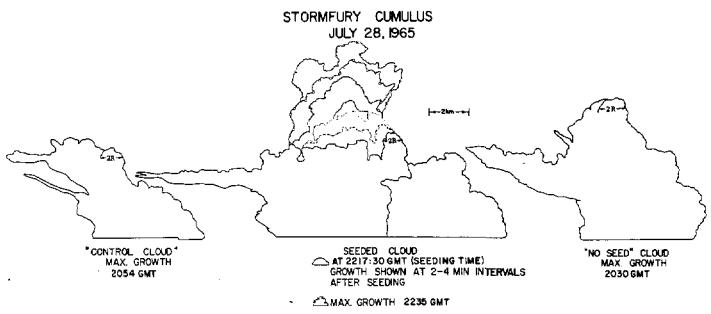

FIGURE 12.—Scale outlines of seeded and control clouds on July 28, 1965, constructed using photogrammetry as described by Simpson (1967).

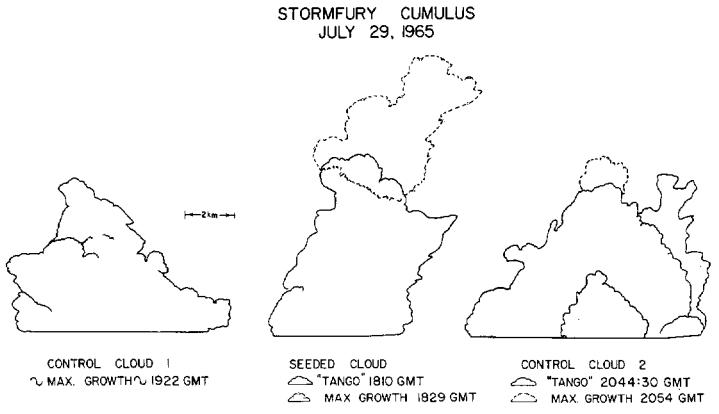

FIGURE 13.—Scale outlines of seeded and control clouds on July 29, 1965, constructed in the same manner as figure 12.

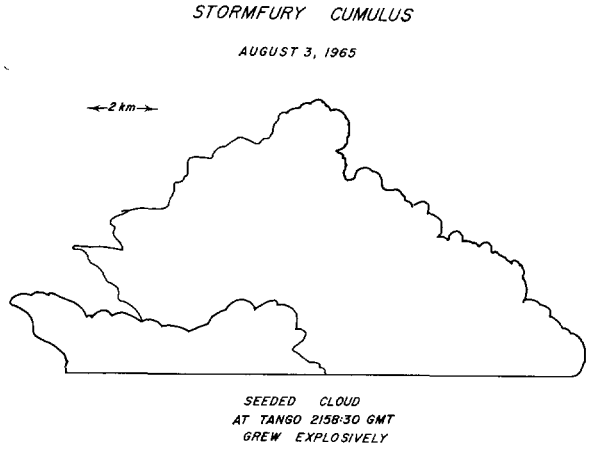

FIGURE 14.—Scale outline of seeded cloud 6, Aug. 3, 1965, at time of seeding. Due to aircraft radar failure, no photogrammetry was possible after seeding.

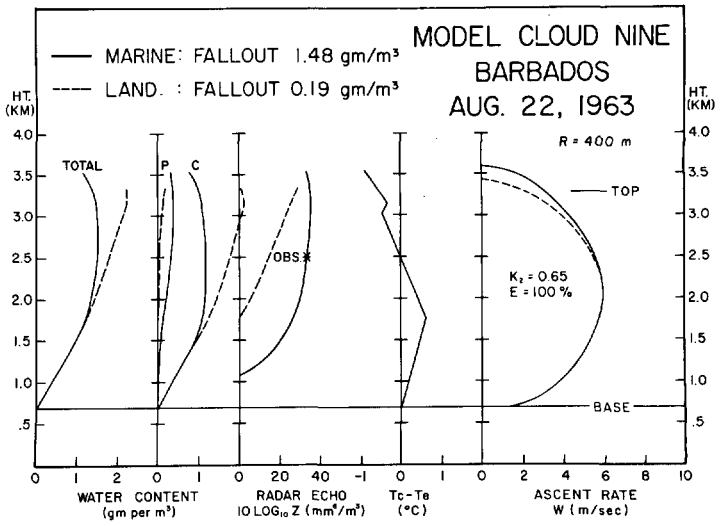

FIGURE 15.—Model cloud 9 for Barbados, Aug. 22, 1963. Model used was EMB 68K, with Berry marine (solid) and Berry land (dashed) autoconversion. Radius data, observed radar echo, and top heights obtained from original records of Saunders (1965). The Barbados radiosonde for 1823 GMT was used. The tower was followed by Saunders between 1802–1817 GMT.

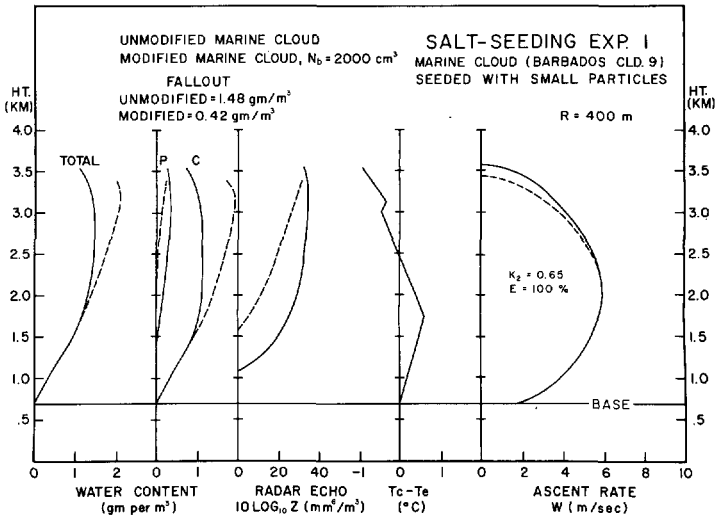

FIGURE 16.—Hypothetical salt seeding experiment 1. Solid lines denote unmodified cloud. Dashed lines denote modified cloud. Attempt to convert maritime toward continental cloud by addition of small particles to make $N_b = 2000$ per cm³. Relative dispersion unchanged from 0.366. Note reduced precipitation production and fallout.

is possible to predict with this model favorable and unfavorable situations for silver-iodide seeding. The favorable situations are those of large vertical growth following seeding or large seeding effect, particularly if explosive growth occurs. The difference between explosive and cut-off tower growth can now be foretold in part, at least, from the model. The less favorable or unfavorable situations for seeding are those with high natural cloud growth and small seedability.

Hygroscopic seeding of warm clouds appears to be an interesting and promising experimental series to test in the field on individual clouds. Several groups, particularly Howell and Lopez (1968), have such experiments underway. However, from both the cloud study and large-scale viewpoint, silver-iodide experiments on supercooled clouds probably have more to offer, in that the dynamics of single clouds and probably of whole cloud groups can be

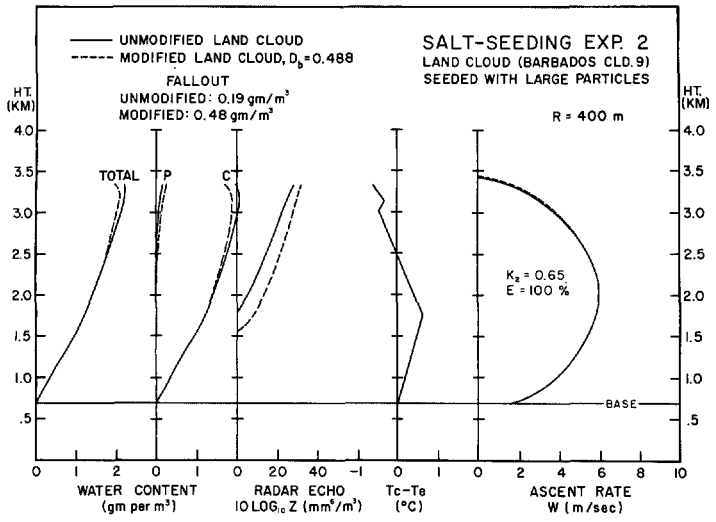

FIGURE 17.—Hypothetical salt seeding experiment 2. Attempt to convert continental toward maritime cloud by addition of large particles. Relative dispersion is increased from 0.146 to 0.488, while N_b remains 2000 per cm³. Note small but percentually significant increase in precipitation production and fallout.

drastically altered; this quite possibly can trigger persistent alterations in the physical cloud processes, such as precipitation structure and fallout.

Note added in proof—Some observational evidence on the hydrometeor spectrum in the ice phase has become available since completion of this paper. During a Florida cumulus seeding experiment in May 1968, it was found that while the slope of the ice particle spectrum did not differ much from the Marshall-Palmer relation used herein, the intercept n_0 (Takeuchi, 1969) was about one order of magnitude higher than that given in table 2.

In our model, n_0 appears to the 0.125 power in the collection equation (11) and the terminal velocity equation (12). An order of magnitude increase in n_0 would, therefore, lead to a collection rate multiplied by a factor of 1.33 and a particle terminal velocity divided by this factor, other parameters and variables being equal.

Let us consider the effect of the higher n_0 on model EMB 68K, which gave the best fit with observations. In this version of the model, the ice collection efficiency E was one, while the ice terminal velocity was reduced to 20 percent of the corresponding values for water. With n_0 increased by the 10 factor, we would obtain the same results as in 68K if we reduce the ice collection efficiency to two-thirds the water value and take the terminal velocities for ice to be 30 percent of those for water particles the same size. These changes appear quite reasonable. Unfortunately, no adequate measurements of either ice collection efficiencies or terminal velocities yet exist to test these inferences.

ACKNOWLEDGMENTS

The authors gratefully acknowledge the valuable help of their colleagues Roscoe Braham, Robert Ruskin, and Helmut Weickmann. They are particularly grateful to Edwin Kessler, upon whose fine work much of this approach is based and to Edwin X. Berry who worked closely with us on autoconversion. Mr. Robert Powell ably drafted the figures, and Mrs. Peggy Lewis prepared the numerous versions of the manuscript.

The work on warm cloud experiments has been kindly supported by the Bureau of Reclamation, U.S. Department of the Interior.

REFERENCES

Andrews, D. A., "Some Effects of Cloud Seeding in Cumulus Dynamics," M. A. thesis, Department of Meteorology, University of California, Los Angeles, **1964**, 139 pp.

Arnason, G., Greenfield, R. S., and Newburg, E. A., "A Numerical Experiment in Dry and Moist Convection Including the Rain Stage," *Journal of the Atmospheric Sciences*, Vol. 25, No. 3, May **1968**, pp. 404–415.

Austin, P. M., "Radar Measurements of the Distribution of Precipitation in New England Storms," *Proceedings of the 10th Weather Radar Conference, Washington, D.C., April 22–25, 1963*, American Meteorological Society, Apr. **1963**, pp. 247–254.

Battan, L. J., and Reitan, C. H., "Droplet Size Measurements in Convective Clouds," *Artificial Stimulation of Rain, Proceedings of the First Conference on the Physics of Cloud and Precipitation Particles, Woods Hole Oceanographic Institution, Woods Hole, Massachusetts, September 7–10, 1955*, Pergamon Press, New York, **1957**, pp. 184–191.

Berry, E. X., "Cloud Droplet Growth by Collection," *Journal of the Atmospheric Sciences*, Vol. 24, No. 6, Nov. **1967**, pp. 688–701.

Berry, E. X., "Modification of the Warm Rain Process," *Proceedings of the First National Conference on Weather Modification, Albany, New York, April 28–May 1, 1968*, American Meteorological Society, State University of New York, Albany, **1968***a*, pp. 81–85.

Berry, E. X., Desert Research Institute, University of Nevada, Reno, **1968***b*, (personal conversation).

Bethwaite, F. D., Smith, E. J., Warburton, J. A., and Heffernan, K. J., "Effects of Seeding Isolated Cumulus Clouds With Silver Iodide," *Journal of Applied Meteorology*, Vol. 5, No. 4, Aug. **1966**, pp. 513–520.

Braham, R. R., Jr., "What is the Role of Ice in Summer Rain-Showers?," *Journal of Atmospheric Sciences*, Vol. 21, No. 6, Nov. **1964**, pp. 640–645.

Braham, R. R., Jr., "Meteorological Bases for Precipitation Development," *Bulletin of the American Meteorological Society*, Vol. 49, No. 4, Apr. **1968***a*, pp. 343–353.

Braham, R. R., Jr., Department of Geophysical Sciences, University of Chicago, **1968***b*, (personal conversation).

Byers, H. R., *Elements of Cloud Physics*, University of Chicago Press, **1965**, 191 pp.

Davis, M. H., and Sartor, J. D., "Theoretical Collision Efficiencies for Small Cloud Droplets in Stokes Flow," *Nature*, Vol. 215, No. 5108, MacMillan (Journals) Ltd., London, Sept. **1967**, pp. 1371–1372.

Gerrish, H. P., and Hiser, H. W., "Mesoscale Studies of Instability Patterns and Winds in the Tropics," *Report* No. 5, Contract No. DA-36-039 SC-89111, University of Miami, Coral Gables, Fla., July **1964**, 55 pp.

Gunn, K. L. S., and Marshall, J. S., "The Distribution With Size of Aggregate Snowflakes," *Journal of Meteorology*, Vol. 15, No. 5, Oct. **1958**, pp. 452–461.

Gunn, R., and Kinzer, G. D., "The Terminal Velocity of Fall for Water Droplets in Stagnant Air," *Journal of Meteorology*, Vol. 6, No. 4, Aug. **1949**, pp. 243–248.

Hosler, C. L., and Hallgren, R. E., "The Aggregation of Small Ice Crystals," *The Physical Chemistry of Aerosols, Discussions of the Faraday Society*, No. 30, The Aberdeen University Press Ltd., Scotland, **1960**, pp. 1–8.

Howell, W. E., and Lopez, M., "Project Rainstart," *Interim Report*, Contract No. NSF-C453, E. Bollay Assoc., Inc., Goleta, Calif., July **1968**, 66 pp.

Kessler, E., III, "Kinematic Relations Between Wind and Precipitation Distributions, I," *Journal of Meteorology*, Vol. 16, No. 6, Dec. **1959**, pp. 630–637.

Kessler, E., III, "Kinematic Relations Between Wind and Precipitation Distributions, II" *Journal of Meteorology*, Vol. 18, No. 4, Aug. **1961**, pp. 510–525.

Kessler, E., III, "Elementary Theory of Associations Between Atmospheric Motions and Distributions of Water Content," *Monthly Weather Review*, Vol. 91, No. 1, Jan. **1963**, pp. 13–27.

Kessler, E., III, "Microphysical Parameters in Relation to Tropical Cloud and Precipitation Distributions and Their Modification," *Geofisica International*, Vol. 5, No. 3, July **1965**, pp. 79–88.

Kessler, E., III, "On the Continuity of Water Substance," *ESSA Technical Memorandum* IERTM–NSSL 33, U.S. Department of Commerce, Washington, D.C., **1967**, 125 pp.

Levine, J., "Spherical Vortex Theory of Bubble-Like Motion in Cumulus Clouds," *Journal of Meteorology*, Vol. 16, No. 6, Dec. **1959**, pp. 653–662.

Levine, J., "The Dynamics of Cumulus Convection in the Trades: A Combined Observational and Theoretical Study," *Ref.* No. 65–43, Woods Hole Oceanographic Institution, Mass., **1965**, 129 pp.

List, R. J., "Smithsonian Meteorological Tables," *Publication* 4014, Smithsonian Institution, Washington, D.C., 6th Rev. Ed., **1951**, 527 pp.

MacCready, P. B., Jr., and Takeuchi, D. M., "Precipitation Mechanisms and Droplet Spectra of Some Convective Clouds," *Analysis of Flagstaff Data, Report* No. 2, Contract No. DA 28–043–AMC–00406(E), Meteorology Research, Inc., Altadena, Calif., **1965**, pp. 3–33.

MacCready, P. B., Jr., and Takeuchi, D. M., "Aircraft Probing of Natural and Seeded Clouds for Project Skyfire," *Final Report*, Meteorology Research, Inc., Altadena, Calif., **1967**, 42 pp.

MacCready, P. B., Jr., and Takeuchi, D. M., "Precipitation Initiation Mechanisms and Droplet Characteristics of Some Convective Cloud Cores," *Journal of Applied Meteorology*, Vol. 7, No. 4, Aug. **1968**, pp. 591–602.

Marshall, J. S., and Palmer, W. McK., "The Distribution of Raindrops With Size," *Journal of Meteorology*, Vol. 5, No. 4, Aug. **1948**, pp. 165–166.

Mason, B. J., "The Physics of Clouds," *Oxford Monographs on Meteorology*, Oxford University Press, London, **1957**, 421 pp.

McCarthy, J., "Computer Model Comparisons of Seeded and Not-Seeded Convective Cloud Depth Using Project Whitetop Data," *Proceedings of the First National Conference on Weather Modification, Albany, New York, April 28–May 1, 1968*, American Meteorological Society, State University of New York, Albany, **1968**, pp. 270–279.

Mee, T. R., and Takeuchi, D. M., "Natural Glaciation and Particle Size Distribution in Marine Tropical Cumuli," *Final Report* Contract No. E22–30–68(N), Meteorological Research, Inc., Altadena, Calif., Aug. **1968**, 71 pp.

Murray, F. W., and Hollinden, A. B., "The Evolution of Cumulus Clouds: A Numerical Simulation and Its Comparison Against Observations," *Final Report*, Contract Nonr–4715(00), Douglas Aircraft Co., Inc., Santa Monica, Calif., Mar. **1966**, 149 pp.

Ogura, Y., "The Evolution of a Moist Convective Element in a Shallow, Conditionally Unstable Atomsphere: A Numerical Calculation," *Journal of Atmospheric Sciences*, Vol. 20, No. 5, Sept. **1963**, pp. 407–424.

Ruskin, R. E., "Measurements of Water-Ice Budget Changes at −5C in AgI-Seeded Tropical Cumulus," *Journal of Applied Meteorology*, Vol. 6, No. 1, Feb. **1967**, pp. 72–81.

Saunders, P. M., "The Thermodynamics of Saturated Air: A Contribution to the Classical Theory," *Quarterly Journal of the Royal Meteorological Society*, Vol. 83, No. 357, July **1957**, pp. 342–350.

Saunders, P. M., "Some Characteristics of Tropical Marine Showers," *Journal of Atmospheric Sciences*, Vol. 22, No. 2, Mar. **1965**, pp. 167–175.

Sax, R. I., "The Importance of Natural Glaciation on the Modification of Tropical Maritime Cumuli by Silver Iodide Seeding," *Journal of Applied Meteorology*, Vol. 8, No. 1, Feb. **1969**, pp. 92–104.

Shafrir, U., and Neiburger, M., "Collision Efficiencies of Two Spheres Falling in a Viscous Medium," *Journal of Geophysical Research*, Vol. 68, No. 13, July 1, **1963**, pp. 4141–4148.

Simpson, J., "Photographic and Radar Study of the Stormfury 5 August 1965 Seeded Cloud," *Journal of Applied Meteorology*, Vol. 6, No. 1, Feb. **1967**, pp. 82–87.

Simpson, J., Brier, G. W., and Simpson, R. H., "Stormfury Cumulus Seeding Experiment 1965: Statistical Analysis and Main Results," *Journal of Atmospheric Sciences*, Vol. 24, No. 5, Sept. **1967**, pp. 508–521.

Simpson, J., Simpson, R. H., Andrews, D. A., and Eaton, M .A., "Experimental Cumulus Dynamics," *Reviews of Geophysics*, Vol. 3, No. 3, Aug. **1965**, pp. 387–431.

Simpson, J., Simpson, R. H., Stinson, J. R., and Kidd, J. W., "Stormfury Cumulus Experiments: Preliminary Results 1965," *Journal of Applied Meteorology*, Vol. 5, No. 4, Aug. **1966**, pp. 521–525.

Simpson, J., Wiggert, V., and Mee, T. R., "Models of Seeding Experiments on Supercooled and Warm Cumulus Clouds," *Proceedings of the First National Conference on Weather Modification, Albany, New York, April 28–May 1, 1968*, American Meteorological Society, State University, Albany, **1968**, pp. 251–269.

Sloss, P. W., "An Empirical Examination of Cumulus Entrainment," *Journal of Applied Meteorology*, Vol. 6, No. 5, Oct. **1967**, pp. 878–881.

Squires, P., "The Microstructure and Colloidal Stability of Warm Clouds: Pt. 1. The Relation Between Structure and Stability, Pt. 2. The Causes of the Variations in Microstructure," *Tellus*, Vol. 10, No. 2, May **1958**, pp. 256–271.

Stommel, H., "Entrainment of Air Into a Cumulus Cloud," *Journal of Meteorology*, Vol. 4, No. 3, June **1947**, pp. 91–94.

Takeuchi, D. M., "Analyses of Hydrometeor Sampler Data for ESSA Cumulus Experiments, Miami, Florida, May 1968," *Final Report*, Contract E22–28–69(N), Meteorology Research, Inc., Altadena, Calif., **1969**.

Telford, J. W., "A New Aspect of Coalescence Theory," *Journal of Meteorology*, Vol. 12, No. 5, Oct. **1955**, pp. 436–444.

Todd, C. J., "Ice Crystal Development in a Seeded Cumulus Cloud," *Journal of Atmospheric Sciences*, Vol. 22, No. 1, Jan. **1965**, pp. 70–78.

Turner, J. S., "The 'Starting Plume' in Neutral Surroundings," *Journal of Fluid Mechanics*, Vol. 13, No. 3, July **1962**, pp. 356–368.

Turner, J. S., "The Motion of Buoyant Elements in Turbulent Surroundings," *Journal of Fluid Mechanics*, Vol. 16, No. 1, May **1963**, pp. 1–16.

Turner, J. S., Department of Applied Mathematics and Theoretical Physics, Kings College, Cambridge, England, **1964**, (personal conversation).

Twomey, S., "The Nuclei of Natural Cloud Formation: Pt. 2. The Supersaturation in Natural Clouds and the Variation of Cloud Droplet Concentration," *Geofisica Pura e Applicata*, Vol. 43, May/Aug. **1959**, pp. 243–249.

Twomey, S., "Statistical Effects in the Evolution of a Distribution of Cloud Droplets by Coalescence," *Journal of Atmospheric Sciences*, Vol. 21, No. 5, Sept. **1964**, pp. 553–557.

Weickmann, H. K., "A Nomogram for the Calculation of Collision Efficiencies," *Artificial Stimulation of Rain, Proceedings of the First Conference on the Physics of Cloud and Precipitation Particles, Woods Hole Oceanographic Institution, Woods Hole, Massachusetts. September 7–10, 1955*, Pergamon Press, New York, **1957**, pp, 161–166.

Weinstein, A. I., and Davis, L. G., "A Parameterized Numerical Model of Cumulus Convection," *Report* No. 11, Contract No. NSF GA–777, The Pennsylvania State University, University Park, May **1968**, 44 pp.

Wexler, R., "Radar Detection of a Frontal Storm 18 June 1946," *Journal of Meteorology*, Vol. 4, No. 1, Feb. **1947**, pp. 38–44.

Woodley, W. L., "Computations on Cloud Growth Related to the Seeding of Tropical Cumuli," *Bulletin of the American Meteorological Society*, Vol. 47, No. 5, May **1966**, pp. 384–392.

[*Received October 31, 1968; revised January 6, 1969*]